Isolation and retrieval of circulating tumor cells using centrifugal forces

Han Wei Hou, Majid Ebrahimi Warkiani, Bee Luan Khoo, Zi Rui Li, Ross A. Soo, Daniel Shao-Weng Tan, Wan-Teck Lim, Jongyoon Han, Ali Asgar. S. Bhagat and Chwee Teck Lim

Supplementary information

Table S1: List of healthy samples as controls.

Healthy Sample No.	Volume processed (mL)	CTCs/mL
1	3	0.67
2	3	0.33
3	3	0.33
4	3	1.33
5	3	0.67
6	3	0.67
7	3	0.67
8	3	0.67
9	3	1.33
10	3	0.33
11	3	0.33
12	3	0.67
13	3	0.67
14	3	0.67
15	3	0.33
16	3	0.33
17	3	0.67
18	3	0.33
19	3	1.33
20	3	0.67

Table S2: Clinico-pathological characteristics of metastatic lung cancer patients who provided samples for CTC enumeration.

Patient Sample No.	Age	Gender	Histology	Cancer stage	Receiving Treatment	CTCs/mL
1	58	M	Small cell carcinoma	IV	Yes	14
2	68	M	Small cell carcinoma	IV	Yes	11
3	51	F	Squamous cell carcinoma	IIIB	No	88
4	62	M	Squamous cell carcinoma	IV	Yes	69
5	57	M	Squamous cell carcinoma	IV	Yes	5
6	53	M	Squamous cell carcinoma, poorly differentiated	IIIA	Yes	59
7	59	M	Papillary adenocarcinoma	IV	Yes	54
8	69	M	Adenocarcinoma with mixed subtypes, well differentiated	IV	Yes	35
9	61	M	Poorly differentiated adenocarcinoma	IV	Yes	26
10	41	F	Squamous cell carcinoma	IV	Yes	81
11	41	F	Adenocarcinoma	IV	Yes	20
12	55	F	Adenocarcinoma	IV	Yes	23
13	45	M	Adenocarcinoma	IV	Yes	25
14	75	M	Adenocarcinoma	IV	No	61
15	62	F	Adenocarcinoma	IV	No	53
16	56	F	Adenocarcinoma	IV	No	11
17	74	M	Adenocarcinoma	IV	No	26
18	66	M	Adenocarcinoma	IV	No	50
19	51	M	Adenocarcinoma	IV	No	52
20	51	M	Adenocarcinoma	IV	No	19

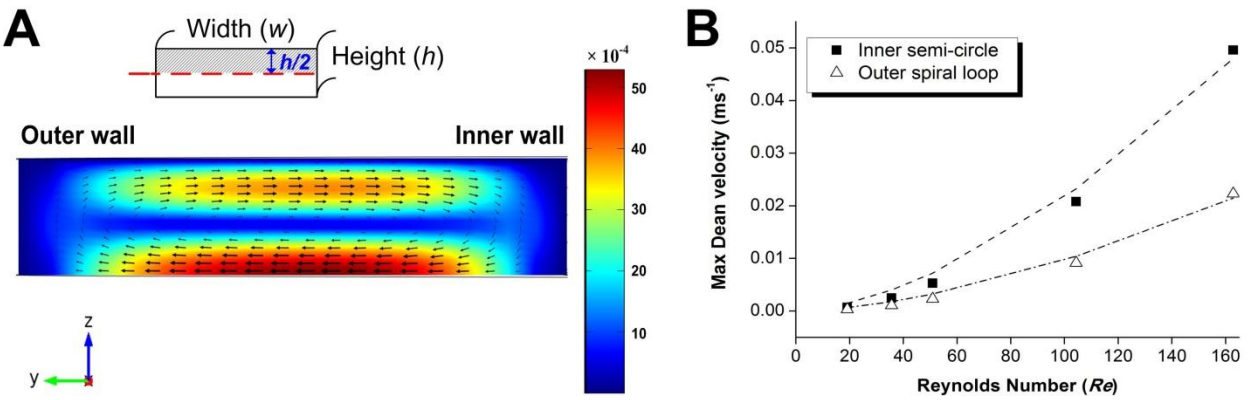

Figure S1. COMSOL modeling of Dean flow in the proposed spiral device. (**A**) Velocity contour plot of the transverse Dean flow at the inner semi-circular channel cross section at Reynolds Number (*Re*) 50.Due to flow symmetry about the middle plane, only the top half of the channel (gray area) was modeled to shorten computational time. Arrows indicate the well-developed transverse Dean flow pattern across the upper half of the channel cross section. Color bar represents Dean velocity magnitude (in m sec^{-1}). (**B**) Plot indicates the maximum Dean flow velocity at different regions of the spiral device at different *Re*. Data points obtained were in good agreement with the fitted curves (dashed lines) based on the power law equation proposed by Ookawara *et al.*[1]**.**

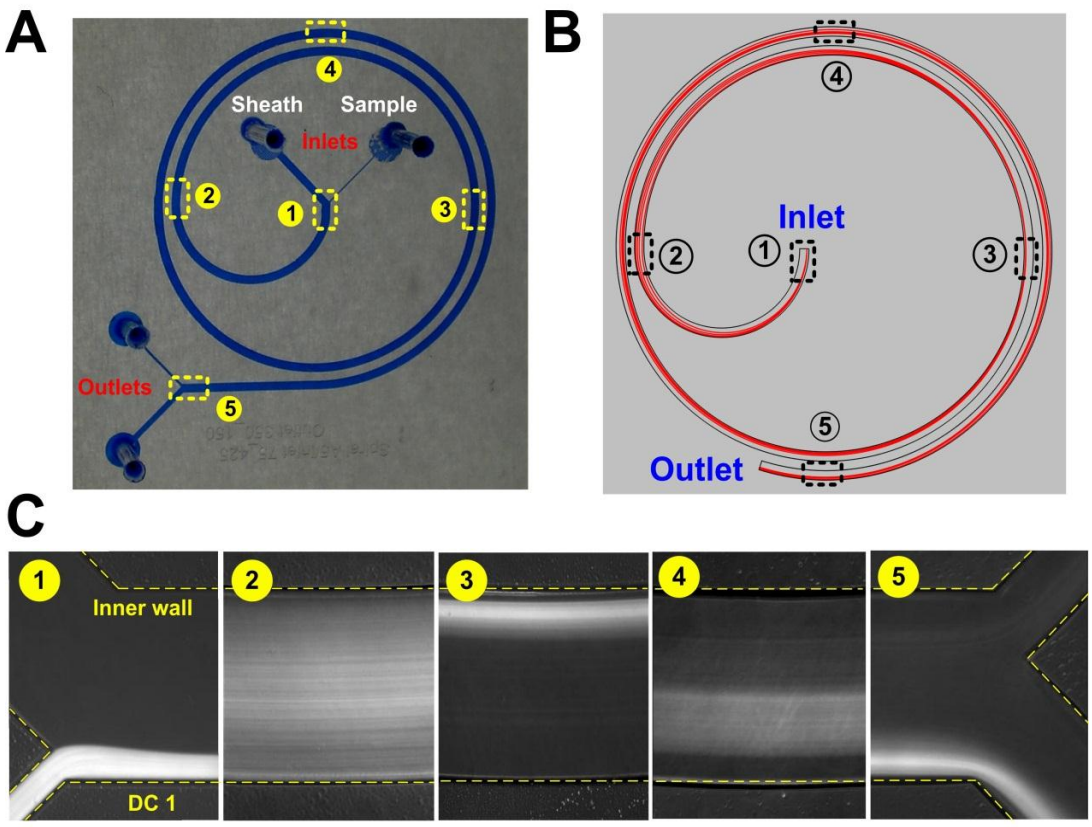

Figure S2. (**A**) Optical image of the spiral microchannel fabricated in PDMS (microchannel is filled with blue dye for visualization). (**B**) Particle tracking (red streamlines) in the modeled spiral device at *Re* 50 (DC 1) indicating the lateral migration of the fluid elements at the outer wall region (inlet) towards the inner wall (position 3) and back to the outer wall again (position 5), thus achieving a complete Dean cycle migration at the end of the channel. (C) Average composite fluorescence images of 3 µm beads ($(a_p)/ h <$ 0.07) equilibrium positions along the channel length illustrating the Dean migration profile at DC 1. Corresponding positions of the captured images are indicated in (**A**). Experimental results were in good agreement with the modeled Dean flow pattern at different positions as shown in (**B**). Dashed yellow lines indicate the approximate channel wall boundaries.

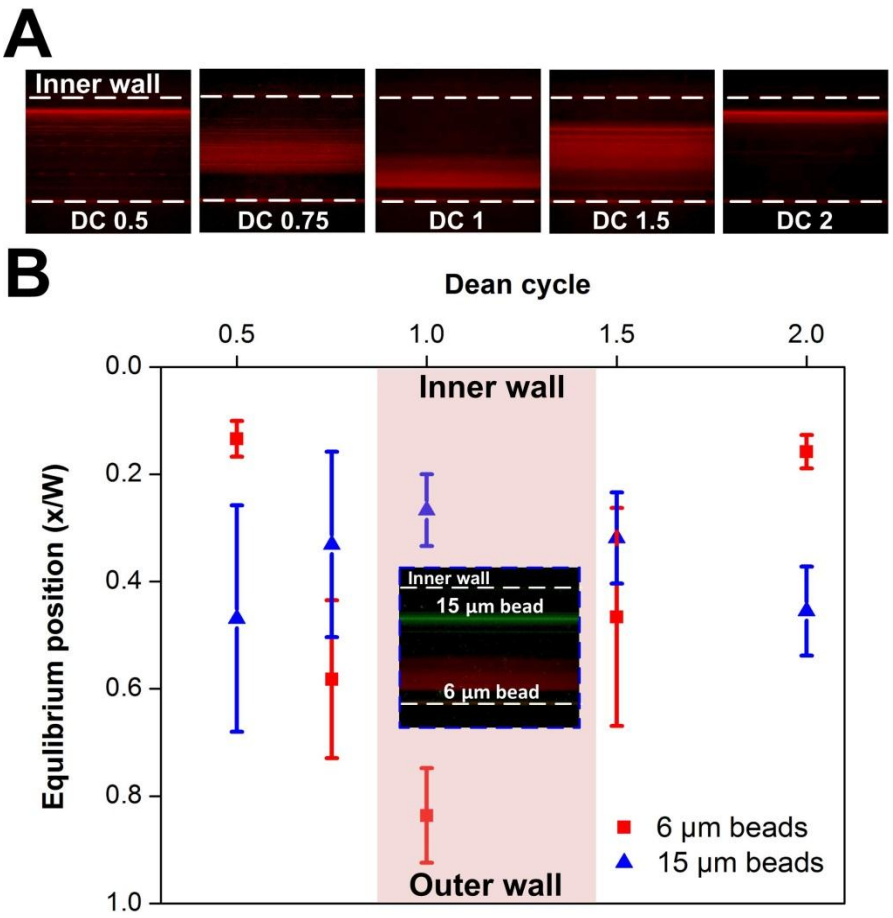

Figure S3. Beads characterization of the spiral microfluidic device at different Dean cycle (DC). (**A**) Average composite fluorescence images indicating equilibrium position of 6 µm beads at different DC (white dotted lines indicate the approximate position of the microchannel walls). (**B**) Plot illustrating the position and width of the focusing bands for 6 µm and 15 µm beads at different DC. Focusing band width is determined by measuring the full width at half maximum (FWHM) of the region occupied by the beads. At DC 1 (pink shaded area), 15 µm beads focused most tightly at the inner wall while 6 µm beads migrated completely to the outer half of the channel, resulting in their complete separation into different outlets. Inset image (blue dotted box) indicates the distinct equilibrium positions for 15 µm and 6 µm beads in a mixed sample at DC 1.

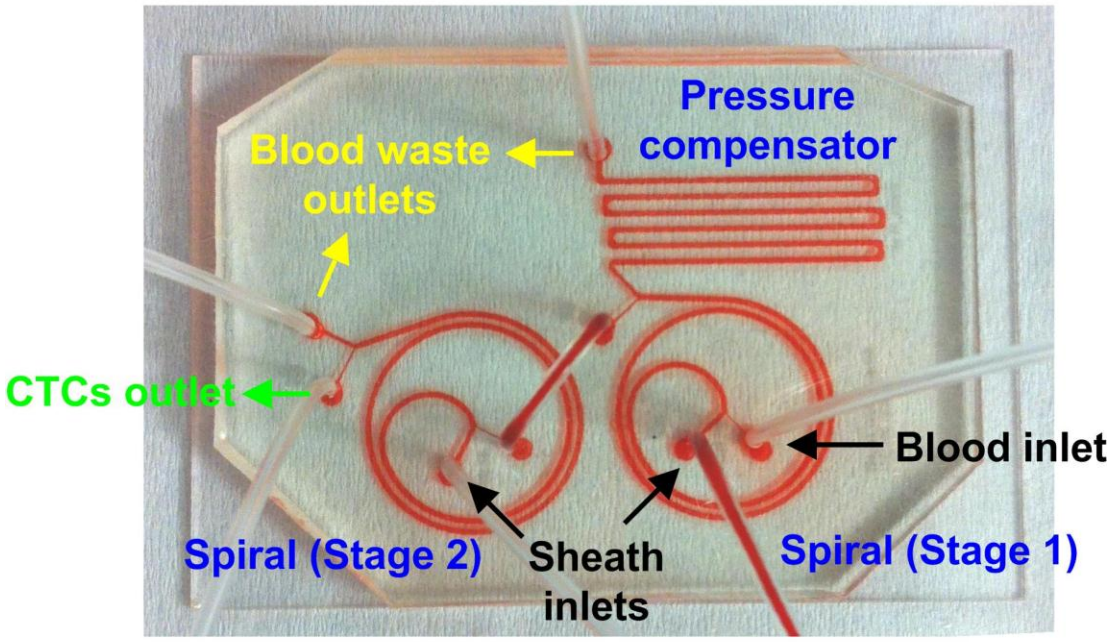

Figure S4. Image of the 2-stage cascaded spiral system by connecting the CTCs outlet of the first spiral device (Stage 1) to the sample inlet of a second spiral device (Stage 2). A pressure compensator was used to account for the additional channel resistance due to the second spiral device.

SI Movie Legends

Movie S1
High speed video (6400 fps) illustrating the separation of MCF-7 cancer cells into the CTCs outlet at the first bifurcation of the cascaded DFF system at DC 1. Sample consists of 20% hematocrit blood sample spiked with high concentration of MCF-7 cells to facilitate video capture. Focused MCF-7 cells (near the inner wall (top side)) are clearly distinguished from RBCs based on morphology and phase contrast.

Movie S2
High speed video (6400 fps) illustrating the 2^{nd} stage separation of MCF-7 cancer cells into the CTCs outlet at DC 1. Remaining RBCs are transposed towards the outer wall and removed through the waste outlet, resulting in complete RBCs removal and separation of MCF-7 cells from 20% hematocrit blood sample with high efficiency (>85%).

References

1. Ookawara, S., Higashi, R., Street, D. & Ogawa, K. Feasibility study on concentration of slurry and classification of contained particles by microchannel. *Chemical Engineering Journal* 101, 171-178 (2004).